PHYSICAL REVIEW B VOLUME 25, NUMBER 12 15 JUNE 1982

Fermi-surface and core-level involvement in conduction-band photoelectron spectroscopy of Na_xWO_3

R. L. Benbow*, M. R. Thuler*, and Z. Hurych
Physics Department, Northern Illinois University, DeKalb, Illinois 69115
(Received 4 February 1982)

Several oscillations observed in the intensity of angle-integrated photoelectron emission from the conduction band of Na_xWO_3 are interpreted to be a consequence of the structure of the multiply connected Fermi surface in the repeated-zone scheme. Other structures are interpreted to be a result of core-hole final-state interactions with the conduction band. In cases where the two processes overlap, additional enhancement is possible.

The occurrence of peaks in angle-integrated ultraviolet photoemission spectroscopy (UPS) with photon energy $h\nu$ has been usually interpreted in terms of one-electron density of states, multielectron effects (satellites, Fano resonances), or atomic-like effects (photoionization cross sections). In this paper we present the observation and interpretation of peaks in angle-integrated UPS which are due to a mechanism not observed previously, namely, the properties of a multiply connected Fermi surface in a repeated-zone scheme. This effect is strong (up to 40% intensity variation) and occurs over a wide photon energy range (10–70 eV) covering regions of strong interband transitions and several possible core-level excitations. The sodium-tungsten bronzes exhibit this effect because of the particular topology of their Fermi surface and narrowness of their conduction band.

The sodium-tungsten bronzes, Na_xWO_3 ($0<x<1$), are nonstoichiometric compounds which exhibit a host of interesting and important x-dependent physical properties. From $0.2\lesssim x \lesssim 0.49$, they are tetragonal and have a superconducting transition temperature which depends on x.[1–3] When $x \gtrsim 0.49$, Na_xWO_3 stabilizes in a cubic structure which is actually an incomplete perovskite structure. In this cubic phase the W $5d$ conduction band is narrow and its width is x dependent; it is separated by a gap of ~ 2 eV from the valence band.[4] The principal sheet of the Fermi surface consists of three mutually perpendicular cylinders intersecting at the origin (Γ point) and directed along the [100] axes.[5] A Kohn anomaly (a sharp break in a phonon dispersion curve) occurs in these compounds when the vibrational wave vector just spans the Fermi-surface cylinders.[6] The Kohn anomaly is observed in Na_xWO_3 because so much of the Fermi surface has the same caliper dimension. In this paper we present photoelectron spectra of Na_xWO_3 for $x=0.5$ and 0.7 which show strong oscillatory behavior in the conduction-band emission as a function of the photon energy $h\nu$. Oscillations of this sort, previously unobserved in photoelectron spectroscopy, result from the cylindrical shape of the Fermi surface.

The data were collected at the University of Wisconsin-Madison Synchrotron Radiation Center on a one-meter normal-incidence monochromator (NIM) (10 eV $\leq h\nu \leq$ 40 eV), a two-meter "grasshopper" grazing-incidence monochromator (40 eV $\leq h\nu \leq$ 110 eV), and a toroidal grating monochromator (TGM, 20 eV $\leq h\nu$ 80 eV). Single crystals of Na_xWO_3 ($x=0.5$, 0.7, and 0.79) were cleaved *in situ* at a background pressure of 2×10^{-10} torr. The photoelectrons were energy analyzed with a double-pass cylindrical mirror analyzer (CMA) operated in the angle-integrated mode. The narrow width ($\lesssim 1.0$ eV) of the conduction band (CB) makes study of emissions from the CB most conveniently done in terms of the constant-initial-energy spectroscopy (CIS). A measured CIS represents $h\nu$-dependent emission from the states at the same initial energy—the center of the CB in this case. A CIS is obtained by scanning the kinetic energy E_k of the CMA synchronously with $h\nu$ such that $h\nu - E_k = \phi - E_i$ is constant.[7] E_i is the electron initial energy and ϕ is the work function. For the CB we took $E_i = -0.4$ eV ($E_F = 0.0$). For $h\nu$ larger than 40.0 eV, CIS's were made from closely spaced photoelectron energy distributions (PED's). A set of PED's covering a broader range is shown in Fig. 1. The prominent

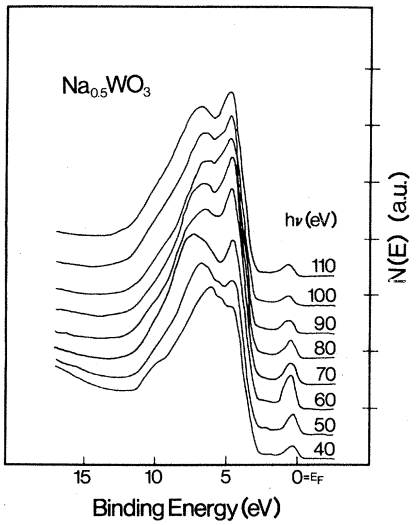

FIG. 1. PED's showing both the valence and conduction band of $Na_{0.5}WO_3$ for 40.0 eV $\leq h\nu \leq$ 110.0 eV at 10.0-eV intervals. The spectra are normalized in the sense that the net integral of the valence-band emission is set equal to a constant. Note the prominence of the conduction-band emission at $h\nu = 60$ eV.

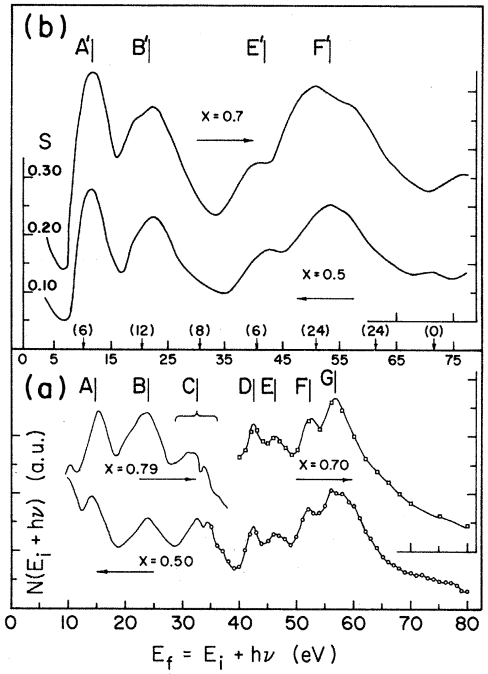

FIG. 2. (a) Solid curve denotes CIS ($E_i - E_F = -0.4$ eV) for $Na_{0.5}WO_3$ and $Na_{0.79}WO_3$; curves with points plotted are interpolated CIS's for $x = 0.5$ and $x = 0.7$, respectively (same initial energy). The normalizations are different so comparisons of intensities of spectra should be made with caution. (b) Fraction S of sphere bounded by Fermi surface. The vertical arrows with numbers in parentheses give numbers of contributions of second and third sheets of Fermi surface. These are for $G = 1.6424$, $g = 0.2300$ (corresponding to $x = 0.5$), and for $G = 1.6356$, $g = 0.3110$ ($x = 0.7$). The value of g was estimated from data of Ref. 6. The overall shape of the curve is not critically sensitive to g.

peak in the CB emission (binding energy ~ 0.4 eV in Fig. 1) shows the sort of intensity modulations the CB emissions go through as a function of $h\nu$. Normalized[8] CIS's in the range $10 \leq E_k \leq 80$ eV are presented in Fig. 2(a). Seven peak structures are labeled A, B, C, D, E, F, and G in the spectra. Feature G corresponds to the CB peak at $h\nu = 60.0$ eV in Fig. 1. Before discussing the origin of these peaks, we note that the features observed in Fig. 2(a) have been present in all samples at the same energies, but differences in the cleaved surfaces cause somewhat differing intensities—even for samples having identical x values.[9]

To account for all peaks in Fig. 2(a), we begin by considering constant-final-energy surfaces defined as follows: If we make the approximation that the final states are free-electron-like, then $E_f = (\hbar^2/2m)\,|\vec{K}|^2$, where $\vec{K}$ is the wave vector of a plane-wave final state, and a sphere of radius $K = |\vec{K}|$ is a constant-energy surface corresponding to E_f. The fraction S of the constant-energy surface which is bounded by the Fermi surface in a repeated-zone scheme is a measure of the number of initial-state electrons available for photoemission from the conduction band. This fraction S varies in an oscillating manner as $h\nu$ and K increase. To see this, consider the two-dimensional projection of the Fermi surface in a repeated-zone scheme in Fig. 3. The circles of radii K_1, K_2, K_3, and K_4 have, respectively, 0.32, 1.00, 0.47, and 0.78 of their arc bounded by the Fermi surface (i.e., lying within the shaded area or within the small dashed-line circles). In this two-dimensional picture, S undulates as K increases. The principal is the same in three dimensions; S for the three-dimensional case for two values of x is plotted in Fig. 2(b). The existence of peaks A', B', E', and F' which show excellent correspondence in energy with similar features in Fig. 2(a) indicates that the interpretation in terms of availability of initial states is generally compatible. We should stress that the only correction included in the calculated curve of Fig. 2(b) is that the energy scale is slightly shifted with respect to that of Fig. 2(a)—a reflection of not including a crystal inner potential. No other correction, e.g., an effective mass, was introduced which would alter the separation of peak po-

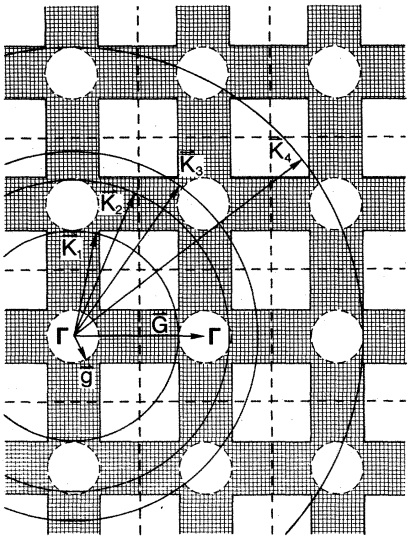

FIG. 3. Two-dimensional projection of Fermi surface (shaded area) in a repeated-zone scheme (dashed lines). The small dashed circles are the cylinders perpendicular to the projection plane. In the figure, $K_1 = G - g$, $\sqrt{2}(G-g) \leq K_2 \leq (G+g)$, $K_3 = \sqrt{2}G$, and $K_4 = 2G + g$, to give (two-dimensional) fractions 0.32, 1.00, 0.47, and 0.78, respectively.

sitions in S.[10]

While the cylinders constitute the principal sheet of the Fermi surface, there are two other closed sheets which we included in the calculation of S.[5] The additional sheets were approximated by concentric spheres (centered at each Γ point) of radii slightly smaller than the cylinder radius g (not indicated in Fig. 3). The contribution to S by these lesser surfaces was of the order of 10–20% of S at any K where they had to be included. The numbers in parentheses above the vertical arrows in Fig. 2(b) show the k location and number of zone centers intersected by our sphere of radius K as a function of E_f. For a comparison of S and the portion of S contributed by the extra sheets of the Fermi surface, see Table I. Although there is a possible contribution from these sheets near peak C, it is clear that they cannot account for the intensity in peak C. Instead, we will argue that the Na $2p$ core level is involved in creating peak C. Further, there are no peaks in Fig. 2(b) corresponding to peaks D and F in Fig. 2(a). Again, these are close in energy to possible zone-center excitations from the secondary sheets of the Fermi surface. There is, however, a close correspondence to the W $5p$ core-level positions and the threshold for these two peaks. This correspondence will be discussed later.

TABLE I. S and portion S_{23} of S due to the smaller sheets of the Fermi surface as a function of E_f. N_{23} is the number of zone centers contributing to S_{23} at E_f.

$\sim E_f$ (eV)	S	S_{23}	N_{23}
10.0	0.24	0.043	6
20.5	0.21	0.043	12
31.0	0.11	0.019	8
41.5	0.16	0.010	6
52.0	0.24	0.030	24
62.0	0.17	0.029	24

There is no shortage of possible core-level excitations which could potentially interact with the conduction electrons. There is the aforementioned Na $2p$ level, as well as the W $4f$ levels and W $5p$ levels. The O $2s$ and the Na $2s$ levels also fall within range of these monochromators. Core-level binding energies are given in Table II. The W $4f$ levels are close to the Na $2p$ level and could be involved with the oscillations in feature C in Fig. 2(a).[11] The Na $2p$ core level is excitonic in Na salts, but Na_xWO_3 is a conductor. If the Na ion in Na_xWO_3 is suitably isolated or screened, the $2p$ core electron might be excited to a pseudoexcitonic state which can undergo direct recombination of the exciton as an alternative to the interatomic Auger decay as shown in Ref. 9. The direct recombination leaves energy $h\nu$ to be either radiated away or else transferred to the crystal. If a conduction electron absorbed all of the energy, the electron would be ejected from the crystal as if it was directly excited by absorbing a photon of energy $h\nu$. This effect was not observed in valence-

TABLE II. Binding energies determined by locating direct emissions relative to the Fermi level for $x = 0.5$. The location of the W $5p_{3/2}$ level was inferred by using the spin-orbit splitting (relative to the W $5p_{1/2}$ level) in Ref. 12 (see also Ref. 14). The energies are given in eV.

O	$2s$	21.65±0.3
Na	$2p$	30.75±0.10
W	$4f_{7/2}$	33.75±0.2
W	$4f_{5/2}$	35.95±0.2
W	$5p_{3/2}$	39.6 ±0.5
W	$5p_{1/2}$	49.5 ±0.5
Na	$2s$	63.85±0.2

band emissions. However, it is not clear if it is because the direct decay mechanism should interact mainly with the electrons (conduction band) closest in energy to the "pseudoexciton," or else that the strong direct valence-band emissions simply overwhelm the modest contribution from the decay mechanism. The valence-band photoemissions are disproportionally stronger than the conduction-band emissions because of differences in the photoexcitation cross sections of W $5d$ and O $2p$ electrons. This difference is inverted at x-ray photoemission spectroscopy (XPS) energies where the $5d$ emissions are stronger than the $2p$ emissions. Since the conduction emissions are suppressed in our photon energy range, the decay of the core level registers just as strongly as the direct photoemission of conduction electrons. The strong valence emissions are barely perturbed by this mechanism.

In the tungsten bronzes, the binding energies of the W $5p$ levels are 39.6 eV ($5p_{3/2}$) and 49.5 eV ($5p_{1/2}$) and are, respectively, 2.9 and 2.6 eV below peaks D and F in Fig. 2(a). The binding energies of the same levels in W metal are about 37.2 and 47.0 eV.[12] The optical-absorption spectrum of W shows two broad structures rising from the two $5p$ thresholds to peaks some 6 eV above the thresholds.[13] The origin of these peaks is thought to lie in multiplet levels of the atomic excitation $5p^6 5d^4 6s^2$ to $5p^5 5d^5 6s^2$ which might subsequently decay to $5p^6 5d^3 6s^2 + e^-$ where the electron has absorbed the energy and may be emitted as a photoelectron. It is processes such as this which cause photoelectron yield spectra to emulate optical-absorption spectra. The multiplet configuration must be complicated with many overlapping components which are not resolved. In Ref. 13 the absorption spectrum of Hf metal is also presented and there is a double-peaked structure rising from each $5p$ core threshold. The initial configuration of Hf is $5p^6 5d^2 6s^2$ which has two fewer $5d$ electrons than W. In the present case the CIS's of Fig. 2(a) show double-peaked structures rising from the $5p$ thresholds more like Hf than W metal. Now we recall that each W ion in the bronze crystal has about one or fewer $5d$ electrons. This more closely approximates Hf metal (two $5d$'s) than W metal (four $5d$'s) and the $5p^6 5d$ excitation to $5p^5 5d^2$ may have a semiresolvable multiplet structure similar to Hf rather than W. There is also the possibility of a resonance with the direct emission of the $5d$ electron. The two processes are:

$$5p^6 5d + h\nu \rightarrow 5p^5 5d^2 \rightarrow 5p^6 + e^- ,$$

and

$$5p^6 5d + h\nu \rightarrow 5p^6 + e^- .$$

To summarize the arguments of the preceding paragraph we can say that the peak pairs D and E and F and G may be due to multiplet structures in the final state involving the $5p$ core hole and the $5d$ electrons whose number has increased by one. We have made an alternate explanation to the proposed Fermi-surface involvement. A fact of the calculation is that feature E' overlaps data peaks D and E collectively which we have attributed to the p-d interactions, and similarly F' with F and G. The p-d interaction does not rule out the Fermi-surface mechanism; the latter will serve to enhance the $5p$ involvement, because more states are available for photoemission at precisely the energies where the $5p$ hole involvement appears. We state without showing that the valence-band CIS's have only very broad and weak structures corresponding to the $5p$ core locations—which indicates that there is no great enhancement of those emissions similar to the conduction-band emissions. Note that the lower portion of the valence band has considerable d character[4] and so would be especially susceptible to the $5p$-$5d$ interaction. The d character in the valence band suggests that some valence electrons are still influenced by the W-ion potential, which allows the average fractional number of $5d$ electrons to exceed x, perhaps even being greater than one. This would make the W ion in the bronzes even more like a Hf atom in Hf metal.

One might argue that a weak $4f$-$5d$ transition could be involved in peak C much as the stronger $5p$-$5d$ interaction is involved in peaks D, E, F, and G. It was effectively argued in Ref. 9 that the structure at 32 eV (peak C) was due to the Na $2p$ level with no observable $4f$ involvement. The likelihood of $4f$ involvement does not seem increased here.

In summary, we have observed peak structures in the conduction-band emissions of Na_xWO_3 for three values of x. We have found excellent correlation between the locations of peaks in experimental data and those predicted by the intersection of constant-energy surfaces with the Fermi surface which results in strong oscillations of the number of initial states available for excitation with increasing $h\nu$. One might, therefore, expect that such peaks could be observed in other solids where the Fermi surface exhibits similar strong anisotropy (e.g., some bronzes, transition-metal oxides, and one- or two-dimensional conductors). In the

present case the possible dominance of the $5p$-$5d$ interactions obscures some of the effects of the multiply connected Fermi surface. Finally, we note that it would be interesting to find a system having a similar Fermi-surface topology but with fewer competing processes so that the Fermi-surface effect can be suitably verified over a broad photon energy range.

This work is supported by NSF Grant No. DMR 81-08302. The experiment was performed at the University of Wisconsin-Madison Synchrotron Radiation Center, which is supported by NSF Grant No. DMR 80-20164.

---

*Mailing address of these authors is: Synchrotron Radiation Center, University of Wisconsin-Madison, 3725 Schneider Drive, Stoughton, Wisconsin 53589.

[1]H. R. Shanks, Solid State Commun. 15, 753 (1974).

[2]C. J. Raub, A. R. Sweedler, M. A. Jensen, S. Broadston, and B. T. Matthias, Phys. Rev. Lett. 13, 746 (1964).

[3]K. L. Ngai and R. Silberglitt, Phys. Rev. B 13, 1032 (1976).

[4]L. Kopp, B. N. Harmon, and S. H. Liu, Solid State Commun. 22, 667 (1977).

[5]L. F. Mattheiss, Phys. Rev. 181, 987 (1969). The Fermi surface of ReO_3 presented in this reference is of the same shape as Na_xWO_3.

[6]W. A. Kamitakahara, B. N. Harmon, J. G. Taylor, L. Kopp, and H. R. Shanks, Phys. Rev. Lett. 36, 1393 (1976).

[7]G. J. Lapeyre, J. Anderson, P. L. Gobby, and J. A. Knapp, Phys. Rev. Lett. 33, 1290 (1974).

[8]The CIS's for $h\nu \lesssim 35$ eV were obtained in continuous synchronous scans of a normal-incidence monochromator and CMA and subsequently corrected for the energy dependence of the photon flux and enhanced with a factor of $E^{3/2}$ as an attempt to negate attenuation of emissions caused by an energy-dependent escape depth (see Ref. 9). The CIS's for $h\nu \lesssim 40$ eV were assembled from photoelectron energy distributions as mentioned in the text. For these we have plotted the integral of the conduction band as the CIS emission, normalized to monochromator flux. On the NIM the flux is taken to be proportional to a sodium-salicylate fluorescence yield. On the TGM and Grasshopper the flux is taken to be proportional to the photoelectron yield of a gold diode divided by the absolute yield of gold (from Dr. C. G. Olson).

[9]R. L. Benbow and Z. Hurych, Phys. Rev. B 17, 4527 (1978).

[10]We are not trying to imply that actual constant-final-energy surfaces are really spheres, but it is difficult to believe that such surfaces are other than cubic distortions to spheres.

[11]The signal-to-noise ratio for the data in this region (collected on the NIM) is relatively low, so these features are not clearly valid data features. On the TGM these features seem to be present, but second-order radiation tends to confuse the issue.

[12]R. Nyholm, A. Berndtsson, and N. Mårtenssen, J. Phys. C 13, L1091 (1980).

[13]J. H. Weaver and C. G. Olson, Phys. Rev. B 14, 3251 (1976).

[14]J.-N. Chazalviel, M. Campagna, G. K. Wertheim, and H. R. Shanks, Phys. Rev. B 16, 697 (1977).